

Fast Polar and Spherical Fourier Descriptors for Feature Extraction

Zhuo YANG^{†a)}, Nonmember and Sei-ichiro KAMATA^{†b)}, Member

SUMMARY Polar Fourier Descriptor(PFD) and Spherical Fourier Descriptor(SFD) are rotation invariant feature descriptors for two dimensional(2D) and three dimensional(3D) image retrieval and pattern recognition tasks. They are demonstrated to show superiorities compared with other methods on describing rotation invariant features of 2D and 3D images. However in order to increase the computation speed, fast computation method is needed especially for machine vision applications like realtime systems, limited computing environments and large image databases. This paper presents fast computation method for PFD and SFD that are deduced based on mathematical properties of trigonometric functions and associated Legendre polynomials. Proposed fast PFD and SFD are 8 and 16 times faster than direct calculation that significantly boost computation process. Furthermore, the proposed methods are also compact for memory requirements for storing PFD and SFD basis in lookup tables. The experimental results on both synthetic and real data are given to illustrate the efficiency of the proposed method.

key words: polar fourier descriptor, spherical Fourier descriptor, rotation invariant, image retrieval, fast algorithm

1. Introduction

Rotation invariant feature extraction is one of the essential challenges in image retrieval and pattern recognition arises from the fact that in many machine vision applications, images should be considered to be the same even if they are rotated. Fourier analysis is very important in signal processing and pattern recognition. It has been widely used on shape description [1], [2] and image retrieval [3]–[5]. By applying fourier analysis to polar and spherical coordinates, Polar Fourier Descriptor(PFD) and Spherical Fourier Descriptor(SFD) are proposed as rotation invariant descriptors for analyzing 2D and 3D images and demonstrated to show superiorities compared with other methods [6]. With the orthogonal property, PFD and SFD can characterize the image function using a set of mutually independent descriptors with minimum redundant and maximal discriminant information.

PFD introduced Fourier-Bessel series to image analysis. Fourier-Bessel series is mainly used on physics-related applications [7], [8]. With boundary condition for the basis functions, Fourier-Bessel series for image functions that defined on a finite interval can be obtained. SFD treats the

spherical object as a whole and can more effectively describes 3D image data compared with Spherical Harmonic (SH) method [9] that is widely used in representation and registration of 3D images [10], [11]. PFD and SFD employ 2D and 3D complex transform defined on a circle and sphere. Unfortunately, the coefficients computation involves many Bessel function, associated Legendre polynomials and trigonometric computations that no fast method has been reported to best of our knowledge. The high computational complexity is the constraint for machine vision applications such as realtime systems, limited computing environments and large image databases. Therefore, reduction of the computational complexity for PFD and SFD is very significant.

This paper focuses on fast PFD and SFD. Fast and compact methods to compute the coefficients of PFD and SFD are proposed by using mathematical properties of trigonometric functions and associated Legendre polynomials. The 2D basis function of PFD has symmetry properties with respect to the x axis, y axis, $y = x$ line, $y = -x$ line and origin that can be used for fast computation. The computational complexity of PFD can be reduced by calculating half of the first quadrant. That is only one eighth of the direct calculation. For many machine vision applications, lookup tables for computing the basis functions are usually stored in the memory. Using the proposed method, only one eighth memory is needed compared with the direct calculation. For SFD, similar symmetry properties exist in 3D space. By analyzing the mathematical properties of associated Legendre polynomial, similar with PFD, its computational complexity is reduced by calculating half of the first spherical quadrant which means almost 16 times fast. Memory requirement for SFD lookup tables are also significantly reduced.

The organization of this paper is as follows. The basic theories of PFD and SFD including mathematics descriptions are provided in Sect. 2. The proposed method is presented in Sect. 3 after analyzing the mathematical properties of trigonometric functions and associated Legendre polynomials. In Sect. 4, the performance of the proposed methods for PFD and SFD are compared with direct calculations against both synthetic and real images. The experimental results illustrate that our proposed method is really effective. Finally, Sect. 5 concludes this study.

2. Background

PFD and SFD use the eigenfunctions of the Laplacian that are separable in polar and spherical coordinates as basis

Manuscript received November 6, 2009.

Manuscript revised January 4, 2010.

[†]The authors are with the Graduate School of Information, Production and Systems, Waseda University, Kitakyushu-shi, 808-0135 Japan.

a) E-mail: joel@ruri.waseda.jp

b) E-mail: kam@waseda.jp

DOI: 10.1587/transinf.E93.D.1708

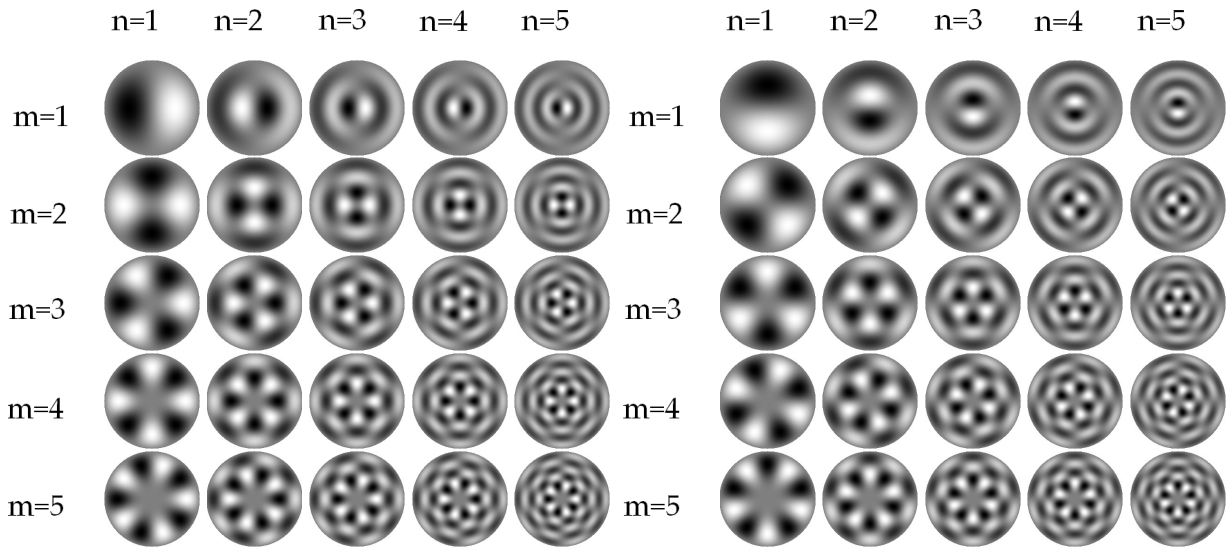


Fig. 1 The basis functions $\Psi_{nm}(r, \varphi)$ of PFD with zero-value boundary condition (Left is real parts and right is imaginary parts).

functions. This section briefly introduces the background of PFD and SFD. For further detail about PFD and SFD, please refer to [6].

2.1 Polar Fourier Descriptor

Given a 2D image function $f(x, y)$, it can be transformed from cartesian coordinates to polar coordinates $f(r, \varphi)$, where r and φ denote radius and azimuth respectively. It is defined on the unit circle that $r \leq 1$, and can be expanded with respect to the basis functions $\Psi_{nm}(r, \varphi)$ as

$$f(r, \varphi) = \sum_{n=1}^{\infty} \sum_{m=-\infty}^{\infty} P_{nm} \Psi_{nm}(r, \varphi), \tag{1}$$

where the coefficient is

$$P_{nm} = \int_0^1 \int_0^{2\pi} f(r, \varphi) \Psi_{nm}^*(r, \varphi) r dr d\varphi. \tag{2}$$

The basis function is given by

$$\Psi_{nm}(r, \varphi) = R_{nm}(r) \Phi_m(\varphi), \tag{3}$$

where

$$R_{nm}(r) = \frac{1}{\sqrt{N_n^{(m)}}} J_m(x_{mn}r), \tag{4}$$

where J_m is the m-th order first class Bessel series [12], and

$$\Phi_m(\varphi) = \frac{1}{\sqrt{2\pi}} e^{im\varphi}. \tag{5}$$

$N_n^{(m)}$ can be deduced by imposing boundary conditions according to the Sturm-Liouville(S-L) theory [13]. Two boundary conditions are interesting. With zero-value boundary condition,

$$N_n^{(m)} = \frac{1}{2} J_{m+1}^2(x_{mn}), \tag{6}$$

where x_{mn} is the nth positive root for $J_m(x)$. With derivative boundary condition,

$$N_n^{(m)} = \frac{1}{2} \left(1 - \frac{m^2}{x_{mn}^2} \right) J_m^2(x_{mn}), \tag{7}$$

where x_{mn} is the nth positive root for $J'_m(x)$.

Rewrite (2) with (3)-(7),

$$P_{nm} = \int_0^1 \int_0^{2\pi} f(r, \varphi) (\cos m\varphi - i \sin m\varphi) R_{nm}(r) r dr d\varphi. \tag{8}$$

$|P_{nm}|$ is rotation invariant and is called Polar Fourier Descriptors (PFD). Fig. 1 show the real and imaginary parts of the basis functions $\Psi_{nm}(r, \varphi)$ under different m, n values with zero-value boundary condition.

2.2 Spherical Fourier Descriptor

After transforming 3D image function $f(x, y, z)$ from cartesian coordinates to spherical coordinates $f(r, \theta, \varphi)$ where r, θ and φ denote the radius, inclination and azimuth respectively. It is defined on the unit sphere that $r \leq 1$, and can be expanded in terms of $\Psi_{nlm}(r, \theta, \varphi)$

$$f(r, \theta, \varphi) = \sum_{n=1}^{\infty} \sum_{l=0}^{\infty} \sum_{m=-l}^l S_{nlm} \Psi_{nlm}(r, \theta, \varphi), \tag{9}$$

where the coefficient is

$$S_{nlm} = \int_0^1 \int_0^{\pi} \int_0^{2\pi} f(r, \theta, \varphi) \Psi_{nlm}^*(r, \theta, \varphi) r^2 \sin \theta dr d\theta d\varphi. \tag{10}$$

The basis function is given by

$$\Psi_{nlm}(r, \theta, \varphi) = \mathbf{R}_{nl}(r)Y_{lm}(\theta, \varphi), \tag{11}$$

where

$$\mathbf{R}_{nl}(r) = \frac{1}{\sqrt{N_n^{(l)}}} j(x_{ln}r), \tag{12}$$

where x_{ln} are positive roots for $j_l(x)$

$$j_l(x) = \sqrt{\frac{\pi}{2x}} J_{l+\frac{1}{2}}(x), \tag{13}$$

and

$$Y_{lm}(\theta, \varphi) = \sqrt{\frac{(2l+1)(l-m)!}{4\pi(l+m)!}} P_{lm}(\cos \theta) e^{im\varphi}, \tag{14}$$

where P_{lm} is the associated Legendre polynomial [13]. Similarly, $N_n^{(l)}$ is determined from S-L boundary conditions. With zero-value boundary condition

$$N_n^{(l)} = \frac{1}{2} j_{l+1}^2(x_{ln}), \tag{15}$$

where x_{ln} is the n th positive root for $j_l(x)$. With derivative boundary condition

$$N_n^{(l)} = \frac{1}{2} \left(1 - \frac{l(l+1)}{x_{ln}^2} \right) j_l^2(x_{ln}), \tag{16}$$

where x_{ln} is the n th positive root for $j_l'(x)$.

Rewrite (10) with (11)-(16),

$$\begin{aligned} S_{nlm} &= \int_0^1 \int_0^\pi \int_0^{2\pi} f(r, \theta, \varphi) P_{lm}(\cos \theta) \\ &(\cos m\varphi - i \sin m\varphi) \sqrt{\frac{(2l+1)(l-m)!}{2\pi(l+m)!}} \\ &\mathbf{R}_{nl}(r) r^2 \sin \theta dr d\theta d\varphi \end{aligned} \tag{17}$$

Spherical Fourier Descriptor (SFD) is defined as

$$\sqrt{\sum_{m=-l}^l |S_{nlm}|}. \tag{18}$$

and is rotation invariant property of the 3D image function for n and l .

3. Fast Polar and Spherical Fourier Descriptors

3.1 Fast PFD

From Eq. (8), we can find for the points on same radius r , the different integrand part for each point is $f(r, \varphi)(\cos m\varphi - i \sin m\varphi)$. As Fig. 2 shown, point (x, y) is a point in first quadrant below $y = x$, has seven other symmetric points with respect to x axis, y axis, $y = x$, $y = -x$ and origin.

Their cartesian and polar coordinates are shown in Table 1.

As known $\sin(\varphi)$ and $\cos(\varphi)$ functions are periodic

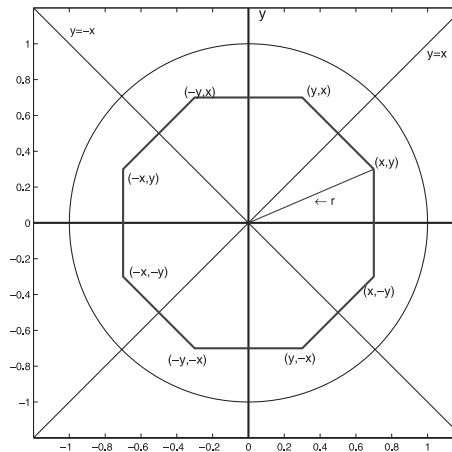


Fig. 2 2D space symmetric points.

Table 1 Symmetric points of (x, y) .

Coordinates	Radius	Azimuth
(x, y)	r	φ
(y, x)	r	$\frac{\pi}{2} - \varphi$
$(-y, x)$	r	$\frac{\pi}{2} + \varphi$
$(-x, y)$	r	$\pi - \varphi$
$(-x, -y)$	r	$\pi + \varphi$
$(-y, -x)$	r	$\frac{3\pi}{2} - \varphi$
$(y, -x)$	r	$\frac{3\pi}{2} + \varphi$
$(x, -y)$	r	$2\pi - \varphi$

functions with period 2π . Periods for $\sin(m\varphi)$ and $\cos(m\varphi)$ are $2\pi/m$. Derived from the periodic and symmetric properties of trigonometric functions that used in FFT [14], mathematical relationships for trigonometric functions exist with respect to different m . For example, if m is divided by 4 with remainder 1 which means $\text{mod}(m, 4) = 1$, following relationship for cosine function can be deduced

$$\cos\left(m\left(\frac{\pi}{2} - \varphi\right)\right) = \sin(m\varphi), \tag{19}$$

$$\cos\left(m\left(\frac{\pi}{2} + \varphi\right)\right) = -\sin(m\varphi), \tag{20}$$

$$\cos(m(\pi - \varphi)) = -\cos(m\varphi), \tag{21}$$

$$\cos(m(\pi + \varphi)) = -\cos(m\varphi), \tag{22}$$

$$\cos\left(m\left(\frac{3\pi}{2} - \varphi\right)\right) = -\sin(m\varphi), \tag{23}$$

$$\cos\left(m\left(\frac{3\pi}{2} + \varphi\right)\right) = \sin(m\varphi), \tag{24}$$

$$\cos(m(2\pi - \varphi)) = \cos(m\varphi). \tag{25}$$

Similar relationships also exist for sinusoidal function and other m values. For the eight symmetric points on the same radius r , if their PFD coefficients can be calculated simultaneously, then the computation time for trigonometric function and Bessel function can be reduced.

Based on foregoing discussion, fast PFD is given by

$$G_m(x, y) = \begin{cases} (f(x, y) + f(y, x) + f(-y, x) + f(-x, y) \\ + f(-x, -y) + f(-y, -x) + f(y, -x) + f(x, -y))\cos(m\varphi) & \text{if } \text{mod}(m, 4) = 0 \\ (f(x, y) - f(-x, y) - f(-x, -y) + f(x, -y))\cos(m\varphi) \\ + (f(y, x) - f(-y, x) - f(-y, -x) + f(y, -x))\sin(m\varphi) & \text{if } \text{mod}(m, 4) = 1 \\ (f(x, y) - f(y, x) - f(-y, x) + f(-x, y) \\ + f(-x, -y) - f(-y, -x) - f(y, -x) + f(x, -y))\cos(m\varphi) & \text{if } \text{mod}(m, 4) = 2 \\ (f(x, y) - f(-x, y) - f(-x, -y) + f(x, -y))\cos(m\varphi) \\ - (f(y, x) - f(-y, x) - f(-y, -x) + f(y, -x))\sin(m\varphi) & \text{if } \text{mod}(m, 4) = 3 \end{cases} \tag{30}$$

$$H_m(x, y) = \begin{cases} (f(x, y) - f(y, x) + f(-y, x) - f(-x, y) \\ + f(-x, -y) - f(-y, -x) + f(y, -x) - f(x, -y))\sin(m\varphi) & \text{if } \text{mod}(m, 4) = 0 \\ (f(x, y) + f(-x, y) - f(-x, -y) - f(x, -y))\sin(m\varphi) \\ + (f(y, x) + f(-y, x) - f(-y, -x) - f(y, -x))\cos(m\varphi) & \text{if } \text{mod}(m, 4) = 1 \\ (f(x, y) + f(y, x) - f(-y, x) - f(-x, y) \\ + f(-x, -y) + f(-y, -x) - f(y, -x) - f(x, -y))\sin(m\varphi) & \text{if } \text{mod}(m, 4) = 2 \\ (f(x, y) + f(-x, y) - f(-x, -y) - f(x, -y))\sin(m\varphi) \\ - (f(y, x) + f(-y, x) - f(-y, -x) - f(y, -x))\cos(m\varphi) & \text{if } \text{mod}(m, 4) = 3 \end{cases} \tag{31}$$

$$FastP_{nm} = \iint_D R_{nm} \left(\sqrt{x^2 + y^2} \right) w(x, y)(G_m(x, y) - iH_m(x, y))dx dy, \tag{26}$$

where

$$D = \{(x, y) | 0 \leq x \leq 1, 0 \leq y \leq x, 0 \leq x^2 + y^2 \leq 1\}, \tag{27}$$

and

$$w(x, y) = \begin{cases} 1 & \text{if } (x, y) \notin K \\ \frac{1}{2} & \text{if } (x, y) \in K \end{cases}, \tag{28}$$

where

$$K = \{(x, y) | y = x, y = -x, x = 0, y = 0\}, \tag{29}$$

and $G_m(x, y)$ and $H_m(x, y)$ are given in Eq. (30) and (31). By using this equation, the whole PFD can be generated by using part of the basic functions. If points located on the symmetry axis K , $w(x, y)$ is applied that the same point is only calculated once. Computational complexity is reduced, only one eighth of the trigonometric and Bessel coefficients are calculated. If we store the coefficients of basis function in lookup table as many machine vision applications usually do, only 12.5% memory is needed compared with the direct calculation.

3.2 Fast SFD

From Eq. (17) we can find that for the points with the same radius r , the different integrand part for each point is $f(r, \theta, \varphi)P_{lm}(\cos \theta)(\cos m\varphi - i \sin m\varphi)$. As Fig. 3 shown, point (x, y, z) in the first spherical quadrant bound with $y = 0$ and $y = x$ planes, has 15 other symmetric points with respect to x axis, y axis, z axis, $y = x$ plane, $y = -x$ plane and origin.

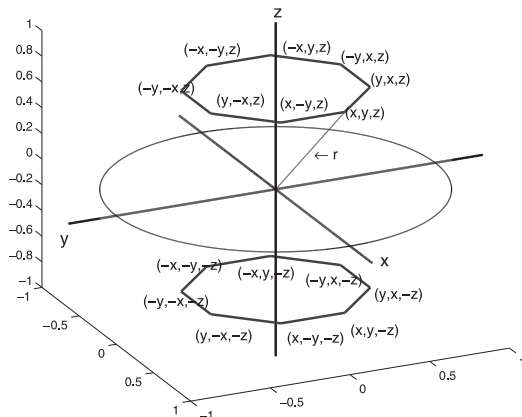


Fig. 3 3D space symmetric points.

Their cartesian and spherical coordinates are show in Table 2.

Mathematical property of associated Legendre polynomial [12] is given by

$$P_{lm}(-x) = \begin{cases} P_{lm}(x) & \text{if } l+m \text{ is even} \\ -P_{lm}(x) & \text{if } l+m \text{ is odd} \end{cases}, \quad (32)$$

for integer l and m .

For two points symmetric with respect to $z = 0$ plane, their inclinations are θ and $\pi - \theta$. By applying mathematical property of associated Legendre polynomial that given in Eq. (32), we have:

$$P_{lm}(\cos(\pi - \theta)) = \begin{cases} P_{lm}(\cos \theta) & \text{if } l+m \text{ is even} \\ -P_{lm}(\cos \theta) & \text{if } l+m \text{ is odd} \end{cases} \quad (33)$$

Inspired by algorithm for PFD, we want to compute all the 16 points simultaneously by using the properties of associated Legendre polynomial and trigonometric function. As the condition of Eq. (30),(31) is different from (33), rewrite (33) as follows,

$$P_{lm}(\cos(\pi - \theta)) = \begin{cases} (-1)^l P_{lm}(\cos \theta) & \text{if } \text{mod}(m, 4) = 0 \\ (-1)^{l+1} P_{lm}(\cos \theta) & \text{if } \text{mod}(m, 4) = 1 \\ (-1)^l P_{lm}(\cos \theta) & \text{if } \text{mod}(m, 4) = 2 \\ (-1)^{l+1} P_{lm}(\cos \theta) & \text{if } \text{mod}(m, 4) = 3 \end{cases} \quad (34)$$

With this property, by combining the eight symmetric points in both up half sphere and down half sphere, fast SFD is given by

Table 2 Symmetric points of (x,y,z).

Coordinates	Radius	Inclination	Azimuth
(x,y,z)	r	θ	φ
(y,x,z)	r	θ	$\frac{\pi}{2} - \varphi$
(-y,x,z)	r	θ	$\frac{\pi}{2} + \varphi$
(-x,y,z)	r	θ	$\pi - \varphi$
(-x,-y,z)	r	θ	$\pi + \varphi$
(-y,-x,z)	r	θ	$\frac{3\pi}{2} - \varphi$
(y,-x,z)	r	θ	$\frac{3\pi}{2} + \varphi$
(x,-y,z)	r	θ	$2\pi - \varphi$
(x,y,-z)	r	$\pi - \theta$	φ
(y,x,-z)	r	$\pi - \theta$	$\frac{\pi}{2} - \varphi$
(-y,x,-z)	r	$\pi - \theta$	$\frac{\pi}{2} + \varphi$
(-x,y,-z)	r	$\pi - \theta$	$\pi - \varphi$
(-x,-y,-z)	r	$\pi - \theta$	$\pi + \varphi$
(-y,-x,-z)	r	$\pi - \theta$	$\frac{3\pi}{2} - \varphi$
(y,-x,-z)	r	$\pi - \theta$	$\frac{3\pi}{2} + \varphi$
(x,-y,-z)	r	$\pi - \theta$	$2\pi - \varphi$

$$\begin{aligned} \text{FastS}_{nlm} &= \iiint_S R_{nl}(\sqrt{x^2 + y^2 + z^2}) \\ &P_{lm}\left(\frac{|z|}{\sqrt{x^2 + y^2 + z^2}}\right) \sqrt{\frac{(2l+1)(l-m)!}{2\pi(l+m)!}} \\ &w(x,y,z)(G_{lm}(x,y,z) - iH_{lm}(x,y,z))dx dy dz \end{aligned}, \quad (35)$$

where

$$S = \{(x,y,z) | 0 \leq x \leq 1, 0 \leq y \leq x, 0 \leq z \leq 1, x^2 + y^2 + z^2 \leq 1\}, \quad (36)$$

and

$$w(x,y,z) = \begin{cases} 1 & \text{if } (x,y,z) \notin A \cup B \\ \frac{1}{2} & \text{if } (x,y,z) \in A \cup B - A \cap B \\ \frac{1}{4} & \text{if } (x,y,z) \in A \cap B \end{cases}, \quad (37)$$

where

$$A = \{(x,y,z) | y = x, y = -x, x = 0, y = 0\}, \quad (38)$$

and

$$B = \{(x,y,z) | z = 0\}, \quad (39)$$

and $G_{lm}(x,y,z)$ and $H_{lm}(x,y,z)$ are given in Eq. (40) and (41). By using this equation, SFD can be generated by only calculating half of the first spherical quadrant. If points located on the symmetry planes A and B , $w(x,y,z)$ is applied that the same point is only calculated once. Computational complexity is reduced, only one sixteenth of the trigonometric function, Bessel function and associated Legendre polynomial coefficients are calculated. If the coefficients need to be stored in lookup table just like many realtime systems usually do, only 6.25% memory is needed.

4. Experimental Results

The performance of the proposed computation method for PFD and SFD in computation reduction is validated through comparative experiments using images of various resolutions. Both synthetic images and real images are used in the experiments. Images with different resolution and content are tested for test to illustrate the efficiency and feasibility of the proposed method over direct calculation. PC environment (Xeon 2.6GHz, 1 G Memory) is used to perform the experiments. Algorithms are implemented by C++ and compiled by gcc 4.3.2 on Linux 2.6.26. GNU Scientific Library [15] is used to calculate Bessel function and associated Legendre polynomials.

4.1 Synthetic Images

In this experiment, synthetic images which are gray scale in format are used. They are generated using the formula given as for 2D PFD,

$$G_{lm}(x, y, z) = \begin{cases} ((f(x, y, z) + f(y, x, z) + f(-y, x, z) + f(-x, y, z) \\ + f(-x, -y, z) + f(-y, -x, z) + f(y, -x, z) + f(x, -y, z)) \\ + (-1)^l(f(x, y, -z) + f(y, x, -z) + f(-y, x, -z) + f(-x, y, -z) \\ + f(-x, -y, -z) + f(-y, -x, -z) + f(y, -x, -z) + f(x, -y, -z)))\cos(m\varphi) & \text{if } \text{mod}(m, 4) = 0 \\ \\ ((f(x, y, z) - f(-x, y, z) - f(-x, -y, z) + f(x, -y, z)) + \\ (-1)^{l+1}(f(x, y, -z) - f(-x, y, -z) - f(-x, -y, -z) + f(x, -y, -z)))\cos(m\varphi) \\ + ((f(y, x, z) - f(-y, x, z) - f(-y, -x, z) + f(y, -x, z)) + \\ (-1)^{l+1}(f(y, x, -z) - f(-y, x, -z) - f(-y, -x, -z) + f(y, -x, -z)))\sin(m\varphi) & \text{if } \text{mod}(m, 4) = 1 \\ \\ ((f(x, y, z) - f(y, x, z) - f(-y, x, z) + f(-x, y, z) \\ + f(-x, -y, z) - f(-y, -x, z) - f(y, -x, z) + f(x, -y, z)) \\ + (-1)^l(f(x, y, -z) - f(y, x, -z) - f(-y, x, -z) + f(-x, y, -z) \\ + f(-x, -y, -z) - f(-y, -x, -z) - f(y, -x, -z) + f(x, -y, -z)))\cos(m\varphi) & \text{if } \text{mod}(m, 4) = 2 \\ \\ ((f(x, y, z) - f(-x, y, z) - f(-x, -y, z) + f(x, -y, z)) + \\ (-1)^{l+1}(f(x, y, -z) - f(-x, y, -z) - f(-x, -y, -z) + f(x, -y, -z)))\cos(m\varphi) \\ - ((f(y, x, z) - f(-y, x, z) - f(-y, -x, z) + f(y, -x, z)) + \\ (-1)^{l+1}(f(y, x, -z) - f(-y, x, -z) - f(-y, -x, -z) + f(y, -x, -z)))\sin(m\varphi) & \text{if } \text{mod}(m, 4) = 3 \end{cases} \tag{40}$$

$$H_{lm}(x, y, z) = \begin{cases} ((f(x, y, z) - f(y, x, z) + f(-y, x, z) - f(-x, y, z) \\ + f(-x, -y, z) - f(-y, -x, z) + f(y, -x, z) - f(x, -y, z)) \\ + (-1)^l(f(x, y, -z) - f(y, x, -z) + f(-y, x, -z) - f(-x, y, -z) \\ + f(-x, -y, -z) - f(-y, -x, -z) + f(y, -x, -z) - f(x, -y, -z)))\sin(m\varphi) & \text{if } \text{mod}(m, 4) = 0 \\ \\ ((f(x, y, z) + f(-x, y, z) - f(-x, -y, z) - f(x, -y, z)) + \\ (-1)^{l+1}(f(x, y, -z) + f(-x, y, -z) - f(-x, -y, -z) - f(x, -y, -z)))\sin(m\varphi) \\ + ((f(y, x, z) + f(-y, x, z) - f(-y, -x, z) - f(y, -x, z)) + \\ (-1)^{l+1}(f(y, x, -z) + f(-y, x, -z) - f(-y, -x, -z) - f(y, -x, -z)))\cos(m\varphi) & \text{if } \text{mod}(m, 4) = 1 \\ \\ ((f(x, y, z) + f(y, x, z) - f(-y, x, z) - f(-x, y, z) \\ + f(-x, -y, z) + f(-y, -x, z) - f(y, -x, z) - f(x, -y, z)) \\ + (-1)^l(f(x, y, -z) + f(y, x, -z) - f(-y, x, -z) - f(-x, y, -z) \\ + f(-x, -y, -z) + f(-y, -x, -z) - f(y, -x, -z) - f(x, -y, -z)))\sin(m\varphi) & \text{if } \text{mod}(m, 4) = 2 \\ \\ ((f(x, y, z) + f(-x, y, z) - f(-x, -y, z) - f(x, -y, z)) + \\ (-1)^{l+1}(f(x, y, -z) + f(-x, y, -z) - f(-x, -y, -z) - f(x, -y, -z)))\sin(m\varphi) \\ - ((f(y, x, z) + f(-y, x, z) - f(-y, -x, z) - f(y, -x, z)) + \\ (-1)^{l+1}(f(y, x, -z) + f(-y, x, -z) - f(-y, -x, -z) - f(y, -x, -z)))\cos(m\varphi) & \text{if } \text{mod}(m, 4) = 3 \end{cases} \tag{41}$$

$$f(i, j) = \text{round}[\text{random}(N, N)], \tag{42}$$

$0 \leq f(i, j) \leq 255, \forall i, j,$

and for 3D SFD,

$$f(i, j, h) = \text{round}[\text{random}(N, N, N)], \tag{43}$$

$0 \leq f(i, j, h) \leq V, \forall i, j, h,$

where $f(i, j)$ and $f(i, j, h)$ are the image function which its

pixels integer in values, $N \times N$ and $N \times N \times N$ are the image resolution and i, j, h are the indices of the image pixels. In this experiment, largest value V of $f(i, j, h)$ equals 255.

These synthetic images are varied in resolution and content. The purpose of using them is to minimize the effects caused by the image and hence robust assessment can be attained from the experimental results. The PFD and SFD

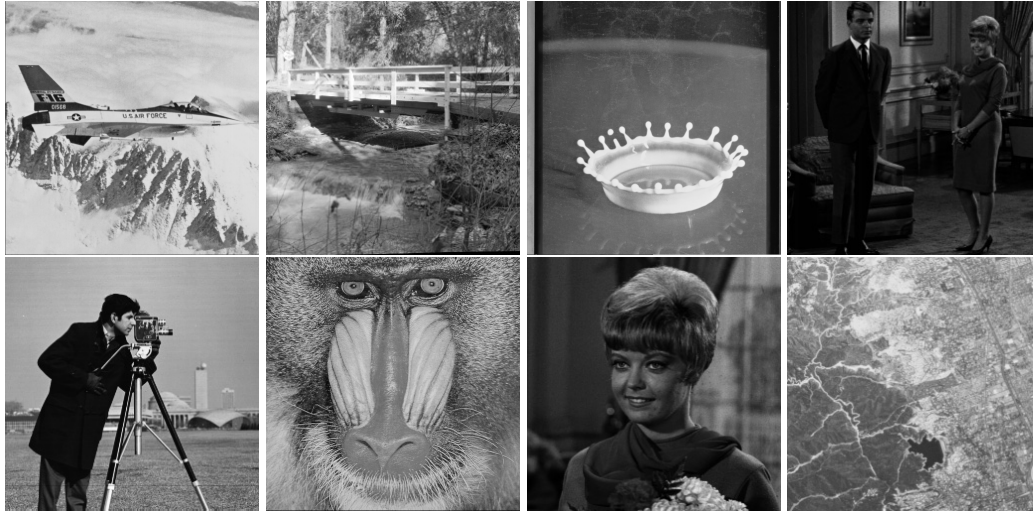


Fig. 4 Real image data set.

Table 3 CPU elapsed time for synthetic images.

Descriptor	Resolution	D	P	P/D
PFD	64*64	0.345	0.045	0.130
	128*128	1.345	0.179	0.133
	256*256	5.561	0.754	0.135
SFD	64*64*64	23.691	1.611	0.068
	128*128*128	117.029	12.392	0.070
	256*256*256	1484.532	101.751	0.069

D=direct calculation, P=proposed method

coefficients are computed from the synthetic images. Direct calculations use Eq. (8) and (17). The proposed methods use Eq. (26) and (35). The maximum number of coefficients calculated for PFD and SFD is 20. With same computation result, but two methods have different running time. Their computation performances in terms of the average CPU elapsed time are given in Table 3.

The results from Table 3 show significant reductions in average CPU elapsed time for PFD and SFD for 2D and 3D images. The average percentage of reduction is around 87.5% and 93.75% for PFD and SFD respectively. Almost similar with the theoretical analysis as Sect. 3.

4.2 Real Images

The performance tests of PFD and SFD computation methods are also carried out for real images. The real images for testing consist of two data sets. 2D test data set consists of 2D real images as shown in Fig. 4. 3D test data set is selected 10 images from Princeton 3D image database [16]. Different numbers of PFD and SFD coefficients are calculated for these two test data sets. The test results are shown in Table 4. Upper part is for 2D test data, lower part is for 3D test data. Proposed method is effective not only for small number coefficients but also for large number coefficients. Based on the results, the reduction trend observed in real images for the proposed method is similar to the reduction trend observed in random images.

Table 4 CPU elapsed time for real image data sets.

Data Set	Coefficients	D	P	P/D
2D images	5	2.832	0.371	0.131
	10	5.689	0.751	0.132
	20	11.398	1.459	0.128
	30	16.829	2.205	0.131
	40	22.563	2.911	0.129
3D images	5	58.097	4.183	0.072
	10	115.014	8.166	0.071
	20	248.368	16.889	0.068
	30	361.181	25.644	0.071
	40	491.766	34.424	0.070

D=direct calculation, P=proposed method

5. Conclusions

In this paper, we propose fast PFD and SFD. By using the symmetric properties and mathematical properties of trigonometric functions and associate Legendre polynomials, the proposed methods only calculate one eighth and sixteenth of trigonometric functions, Bessel functions and associate Legendre polynomials to get PFD and SFD, respectively. That is to say, for 2D images proposed fast PFD computation speed is increased by 8 times. For 3D images, proposed fast SFD method is 16 times faster. Experimental results are also given on both synthetic and real images to illustrate their efficiencies. Moreover the memory requirement for storing the coefficients of basis functions are also reduced. Wide range of machine vision applications that need fast computation of rotation invariant descriptors will benefit from this method.

Acknowledgement

We would like to thank all people providing their free code and test images for this study. This work was supported in part by Grant-in-Aid (No.21500181) for Scientific Research by the Ministry of Education, Science and Culture of Japan.

References

- [1] K. Fu and E. Persoon, "Shape discrimination using Fourier descriptors," *IEEE Trans. Pattern Anal. Mach. Intell.*, vol.PAMI-8, no.3, pp.388–397, 1986.
- [2] D. Zhang and G. Lu, "A comparative study of Fourier descriptors for shape representation and retrieval," *Proc. ACCV2002*, pp.646–651, 2002.
- [3] I. Bartolini, P. Ciaccia, and M. Patella, "Warp: Accurate retrieval of shapes using phase of Fourier descriptors and time warping distance," *IEEE Trans. Pattern Anal. Mach. Intell.*, vol.27, no.1, pp.142–147, 2005.
- [4] D. Zhang and G. Lu, "Shape-based image retrieval using generic Fourier descriptor," *Signal Process., Image Commun.*, vol.17, no.10, pp.825–848, 2002.
- [5] I. Kunttu, L. Lepisto, J. Rauhamaa, and A. Visa, "Multiscale Fourier descriptors for defect image retrieval," *Phys. Rev. Lett.*, vol.27, no.2, pp.123–132, 2006.
- [6] Q. Wang, O. Ronneberger, and H. Burkhardt, "Rotational invariance based on Fourier analysis in polar and spherical coordinates," *IEEE Trans. Pattern Anal. Mach. Intell.*, vol.31, no.9, pp.1715–1722, 2009.
- [7] D. Lemoine, "The Discrete Bessel Transform Algorithm," *J. Chemical Physics*, vol.101, no.5, pp.3936–3944, 1994.
- [8] R. Bisseling and R. Kosloff, "The fast Hankel transform as a tool in the solution of the time dependent Schringer equation," *J. Computational Physics*, vol.59, no.1, pp.136–151, 1985.
- [9] M. Kazhdan, T. Funkhouser, and S. Rusinkiewicz, "Rotation invariant spherical harmonic representation of 3D shape descriptors," *Proc. Symp. Geometry Processing*, pp.167–175, 2003.
- [10] H. Huang, L. Shen, R. Zhang, F. Makedon, A. Saykin, and J. Pearlman, "A novel surface registration algorithm with medical modeling applications," *IEEE Trans. Inf. Technol. Biomed.*, vol.11, no.4, pp.474–482, 2007.
- [11] S. Erturk and T.J. Dennis, "3D model representation using spherical harmonics," *Electron. Lett.*, vol.33, no.11, pp.951–952, 1997.
- [12] L. Andrews, *Special Functions of Mathematics for Engineers*, second ed., SPIE Press, 1997.
- [13] W. Kosmala, *Advanced Calculus: A friendly approach*, Prentice-Hall, 1999.
- [14] C.S. Burrus and T.W. Parks, *DFT/FFT and Convolution Algorithms and Implementation*, John Wiley & Sons, 1985.
- [15] The Gnu Scientific Library, <http://www.gnu.org/software/gsl/>, 2009.
- [16] Princeton 3D image database, <http://shape.cs.princeton.edu/benchmark/>, 2005.



Sei-ichiro Kamata received the M.S. degree in computer science from Kyushu University, Fukuoka, Japan, in 1985, and the Doctor of Computer Science, Kyushu Institute of Technology, Kitakyushu, Japan, in 1995. From 1985 to 1988, he was with NEC, Ltd., Kawasaki, Japan. In 1988, he joined the faculty at Kyushu Institute of Technology. From 1996 to 2001, he has been an Associate Professor in the Department of Intelligent System, Graduate School of Information Science and Electrical Engineering, Kyushu University. Since 2003, he has been a professor in the Graduate School of Information, Production and Systems, Waseda University. In 1990 and 1994, he was a Visiting Researcher at the University of Maine, Orono. His research interests include image processing, pattern recognition, image compression, and space-filling curve application. Dr. Kamata is a member of the IEEE and the ITE in Japan.



Zhuo Yang received the B.E. and M.E. degree in control engineering and software engineering from Beijing Institute of Technology, Beijing, China, in 2005 and 2008 respectively. From 2006 to 2009 he worked in IBM China Development Lab. He is currently a Ph.D student in Graduate School of Information, Production and Systems, Waseda University, Japan. His current research interests are mainly content based image retrieval and pattern recognition.